

**BZBJ1058+5628: a new quasi-periodic BL Lac object  
from the Asiago plate archive**

R. Nesci

Physics Dept., University of Roma La Sapienza,  
Piazzale A. Moro 2, I-00185 Roma, Italy

`roberto.nesci@uniroma1.it`

Received \_\_\_\_\_; accepted \_\_\_\_\_

## ABSTRACT

We present the historic photographic light curves of three little known Blazars (two BL Lacs and one FSRQ), BZB J1058+5628, BZQ J1148+5254 and BZB J1209+4119 spanning a time interval of about 50 years, mostly built using the Asiago plate archive.

All objects show evident long-term variability, over which short-term variations are superposed. One source, BZB J1058+5628, showed a marked quasi-periodic variability of 1 mag on time scale of about 6.3 years, making it one of the few BL Lac objects with a quasi-periodic behavior.

*Subject headings:* galaxies: active — BL Lacertae objects: individual  
(BZBJ1058+5628, BZQJ1148+5254, BZBJ1209+4119)

## 1. Introduction

Long-term ( $\geq 20$  years) optical light curves are still available only for a relatively small number of Active Galactic Nuclei (AGN) and Blazars. Pioneering work in this field was made by several authors (Pica et al. 1988; Webb et al. 1988) on relatively large samples of sources over a time window of about 20 years. For some sources these curves show long-term trends occurring over time scales of decades, while others show only short-term variability.

A few sources had dedicated papers to their long-term optical variability. Among the best studied sources we recall: OQ 530, whose optical brightness faded at 0.035 mag/yr for about one century (Massaro et al. 2004); S5 0716+71, showing a monotonic brightening trend of 0.11 mag/yr of its mean luminosity over the last 40 years (Nesci et al. 2005); ON 231, with a long term decreasing trend of 0.023 mag/yr followed by an increasing one of 0.07 mag/yr (Massaro et al. 2001); WGA 0447.9-0322, with a long monotonic trend of 0.11 mag/yr, similar to S5 0716+71 (Nesci et al. 2007); 5C 3.178 declining at 0.03 mag/yr over 30 years (Sharov 1995).

In some cases a periodicity of the outbursts has also been found, the best case by far being OJ 287 (Sillampaa et al 1988, Valtonen et al. 2009). Other such sources are AO 0235+164, with a possible 5 years period of strong outbursts (Raiteri et al. 2008 and references therein) and S5 0716+71 (Raiteri et al. 2003) with recurrence of about 3 years. Also in the radio band a few sources have shown periodic outbursts (e.g. 3C 454.3, Ciaramella et al. 2004, Qian et al. 2009).

The origin of the fast variations in Blazars is generally explained by the relativistic boosting of perturbations moving down a jet pointing close to the line of sight. The relevant quantity for the boosting is the beaming factor  $\delta = 1 \times (\Gamma \times (1 - \beta \cos\theta))^{-1}$ , where  $\Gamma$  and  $\beta$  are the Lorentz factor and the velocity (in units of the speed of light) of the perturbations' bulk motion and  $\theta$  is the angle between the jet and the line of sight.

On the other hand the nature of secular variations is unclear. A suggestive possibility is that they can be associated with changes in the structure and/or direction of the inner jet (see e.g. Kadler et al. 2006). It is difficult, however, to obtain a clear evidence of such changes because it requires long and accurate multifrequency campaigns with VLBI angular resolution on a sample of several sources: such a study has been done e.g. by Nesci et al. (2005) in the case of S5 0716+71, suggesting that precession of the jet may indeed explain its observed light curve behavior, or Massaro et al. (2004) in the case of OQ 530.

With the successful launch of the Fermi satellite for Gamma ray astronomy, an all-sky monitoring of the Blazars emission has started, which will probably bring to the attention of astronomers a number of poorly known sources. Lists of potential Gamma ray Blazars have been prepared in the framework of the GLAST project by Massaro et al. (2009), containing about 2800 objects, and Sowards-Emmerd et al. (2005), listing about 770 Northern sky sources. For most of these sources very few data exist, basically those allowing their detection and the classification as an AGN. A better knowledge of the properties of these sources will be useful for the interpretation of the Gamma-Ray data now available from the Fermi mission.

To determine the historic light curve of AGNs, an effective way is to use survey plates taken with wide angle instruments, like the Schmidt telescopes, in fields covered over a large time span for patrol of other targets, like Supernovae or variable stars. A good mine of such material is the archive of the Asiago Observatory (<http://dipastro.pd.astro.it/asiago/>), with its two Schmidt instruments, the 67/92cm, operative between 1965 and 1998, and the 40/50 cm, operative between 1958 and 1992.

We selected therefore, from the Massaro et al. (2009) catalogue, those sources for which no historic optical light curve is still published, nominally bright enough to be well measurable on the plates of the 67/92 cm telescope ( $B \leq 17.5$ ), without an obvious strong

host galaxy around, and for which a large ( $\geq 50$ ) number of plates is available spread over a long ( $\geq 10$  years) time interval, so that a meaningful historic light curve can be derived. Unfortunately, a very small number of sources matched these conditions, mainly due to their optical faintness.

In this paper we report the results of our photometric measurements of these plates and the first optical historic light curve for three sources, BZBJ1058+5611, BZQJ1148+5254 and BZBJ1209+4119.

## 2. Photographic data reduction and light curves

Plates were digitized at the Asiago Observatory with an EPSON 1680 Plus scanner, a sampling step of 16 micron (1600 dpi) in grayscale/transparency mode and 16 bit resolution. Plate scanning included also the unexposed borders to measure the plate fog level ( $F$ ). The transformation of the recorded plate transparency  $T$  of each pixel into a relative intensity  $I$  was obtained applying the simple relation  $I = (F - Z)/(T - Z)$ , where  $Z$  is the instrumental zero level. The best way to determine this level is to use the value of the darkest pixel in the center of the most overexposed star.

Most of the plates were with 103aO emulsion and GG13 filter, similar to the IIIaJ+GG385 emulsion+filter combination used in the Second Palomar Sky Survey (POSS II): therefore we established, for each field, a photometric comparison sequence selecting about 20 stars and taking their nominal magnitudes from the GSC2.3 catalogue, using the "J" photometric band, which is based on the POSS II.

Instrumental magnitudes for each plate were obtained using IRAF/APPHOT tasks with a fixed aperture of 3.0 pixels for the 67cm Schmidt plates, corresponding to the FWHM of the average stellar profiles. We checked that the selected stars were not variable.

The sky value was taken from a concentric annulus of 10 pixels inner radius and 10 pixels width, using the "mode" algorithm for the computation.

A calibration curve for each plate was then obtained using the GSC2.3 values of the comparison stars. These curves were reasonably tight but showed a slight departure from a simple linear relation, so we fitted them with a 2nd order polynomial law. The most discrepant star was then automatically excluded and a new, final fit, recomputed.

Having a large number of plates for each field, we performed an intercalibration of our reference stars magnitudes. The differences with respect with the GSC2 values were nearly always smaller than 0.1 mag, indicating that this catalogue is a very good starting point to derive historical photographic light curves. The intercalibrated magnitudes (which we will call B/Asiago) were then used to rebuild the calibration curve for each plate, which were again well fitted by a 2nd order polynomial relation with an appreciably smaller scatter.

The  $B_J$  magnitude of the AGN was then derived from the instrumental one using the calibration curve. The scatter of the points around the fitting curve depends on the plate quality: typical rms errors are 0.1 mag. These errors were adopted as estimates of our photometric accuracy.

A number of plates were taken without filter, so that a proper systematic correction had to be derived. Indeed an AGN is typically bluer than the average field stars and should appear therefore brighter when the UV part of the spectrum is not cut by the blue filter. Unfortunately we did not find plates taken with the two filter/emulsion combinations in the same night (or nearby nights) for our sources. To find the systematic correction between the two combinations, we decided therefore to plot the light curves derived separately from the plates with and without filter and empirically look for a systematic shift between the two. This trick was successful in the case of 1148+52, for which there was a large overlap for the two light curves: the correction was found to be small, about 0.2 mag, and was

adopted for all three sources.

One source (1058+56) was sufficiently bright that could be well detected also on the films taken with the smaller 40/50cm Schmidt telescope. This allowed to extend the light curve back to the years 1962-65. These films were generally unfiltered and had the PANCHRO ROYAL emulsion; very wisely, however, the Observatory policy for the patrol fields taken with the 40/50 Schmidt was to secure sometimes a couple of images taken in the same night with PANCHRO ROYAL and 103aO (unfiltered) emulsion for comparison. We tried to use these couples of films, where the AGN was well exposed, to determine an empirical transformation from PANCHRO ROYAL into 103aO magnitudes, but the intrinsic photometric accuracy of the stars was rather low (0.2 mag) and the number of pairs too small (5) to derive a statistically reliable correction ( $-0.4 \pm 0.2$  mag). Also in this case therefore we overplotted the uncorrected light curves obtained from the 103aO+GG13 plates and from the unfiltered PANCHRO ROYAL films in the years 1965-1968: the systematic shift was derived comparing the average values of the source in the two data sets. The result was found to be in good agreement with that obtained from the 5 plate pairs seen above. Finally the correction from 103aO (unfiltered) into 103aO+GG13 derived from the 67cm plates was applied to derive the final  $B_J$  magnitudes.

For each source a finding chart is given in Fig. 1, 2 and 3, derived from the Asiago plates, where the comparison stars are marked with letters and A is the AGN. Table 1 to 3 give the star flag (column 1), RA and DEC (J2000) derived from the GSC2.3 (column 2 and 3), adopted  $B_J$  magnitude (column 4) and its uncertainty (column 5) derived from the rms scatter in our dataset.

The photometric data of the three AGNs are reported respectively in Tables 5, 6 and 7. We report here just a few lines of Table 5 as example. Column 1 is the plate identification, column 2 is the filter/emulsion, column 3 the JD, column 4 is the rms deviation of the

calibration curve, column 5 the  $B_J$  magnitude. The meaning of column 2 is: none=103aO unfiltered; PANC= Panchro-Royal emulsion without filter; GG13= 103aO+GG13.

The resulting light curves are shown in Fig. 4, 5 and 6.

Two additional points were obtained from the POSS I and POSS II digitized blue plates available on-line (e.g. at the ESO website), using the same comparison stars used for the Asiago plates and IRAF/apphot for aperture photometry. The two POSS plates have different emulsion/filter combination (respectively 103aO unfiltered and IIIaJ+GG395) so the POSS I magnitude was corrected like the Asiago 103aO unfiltered ones.

Another recent literature point can be derived from the Sloan Digital Sky Survey (SDSS, Collinge et al. 2005), if the source is not saturated, converting the  $g$  magnitude into the GSC2.3  $B_J$  scale. A linear fit on a scatter plot of  $B_J$  vs.  $g$  of the comparison stars for each of our fields gave a slope  $\sim 1$  and a small shift in the zero point. We expected however the presence of a small color term, due to the redder passband of the  $g$  filter with respect to the IIIaJ+GG395 combination: given that the AGNs have an  $(u-g)$  color definitely bluer than the average field stars, this term should be appreciable. To this purpose, scatter plots of the  $(u-g)$  vs.  $(g-B_J)$  magnitudes of the comparison stars for each field were made: the correlation however was not very tight, probably due to the lower accuracy of the GSC2.3 magnitudes, and in any case all the stars were substantially redder than the AGN so that a large extrapolation of the linear fit would be required to evaluate the color correction; eventually we preferred to ignore the color effect (which is in any case about 0.1 - 0.2 magnitudes) and just apply the zero-point correction.

We made furthermore in the Summer 2009 a final photometric point for each source using our Vallinfreda 50cm Newtonian telescope and CCD camera with a Marconi 47-10 back-illuminated chip and standard Johnson-Cousins filters.

All these additional photometric points are also reported in the respective Tables.

### 3. Data of Individual Sources

BZBJ1058+5628

The first optical spectrum of this source was published by Marcha et al. (1996) giving a redshift  $z=0.41$  from a strong [O III] emission line. Subsequent spectroscopic observations did not show any more these lines, but only the spectrum of the host galaxy with absorption lines at  $z=0.144$  (Laurent-Muehleisen et al. 1988, Bade et al. 1988). A more recent spectrum can be found in the SDSS (Adelman-McCarthy et al. 2008), which provides the same redshift value ( $z=0.143$ ) from several absorption lines of the host galaxy and the faint  $H\alpha + N[II]$  emission lines. The equivalent width of this blend is about  $5 \text{ \AA}$ , giving a classification of BL Lac to this source. The host galaxy is well evident in the image of the SDSS, but absolutely invisible in the Asiago plates. To evaluate the galaxy contribution in the B band for our source we used the equivalent width of the G-band absorption line. The catalogue of absorption lines of elliptical galaxies (Trager et al. 1998) gives an average value  $5.5 \pm 1.0 \text{ \AA}$  for this feature. The SDSS spectrum of our source has a G-band E.W.= $1.0 \text{ \AA}$ , so that about 80% of the flux is actually due to the blazar component at  $4300 \text{ \AA}$  rest-frame. Due to the redshift, the observed B band is centered on the CaII H and K lines, where the galaxy contribution is still lower, so that the flux variation amplitude is little affected by the stable underlying galaxy contribution.

We found 47 plates with 103aO+GG13 and 25 plates without filter taken with the 67/92 Schmidt, covering the time interval 28-11-1965 to 06-01-1992. Their distribution in time however was not well suited to evaluate the systematic difference between the two combinations. Given the brightness of the source, it was also measurable in several (41

PANCHRO ROYAL, 9 103aO) films of the small Schmidt, allowing us to derive its light curve in the years 1962-65. Films taken during the year 1969 were used to determine the systematic difference between the two filter/emulsion combinations.

The Asiago light curve covers about 11000 days and shows a definite monotonic decreasing trend of 2 magnitudes (0.053 mag/year). Superposed on this trend there are wide oscillations with peak-to-peak amplitude of about 1 mag, with a time scale of about 2500 days (7 years). The Fourier spectrum is dominated by three low frequencies (0.00039, 0.00066 and 0.00082, corresponding to 2550, 1490 and 1220 days) with similar amplitude, but a lot of other frequencies are present with non negligible amplitude. Making a fit of the light curve keeping only the three low frequencies, the amplitude of the 2550 days period is the largest (0.27 mag) followed by 1220 (0.14) and 1490 (0.11), with a rms deviation from the actual light curve of 0.22 mag. The deviations are mainly concentrated in some segments of the light curve, and can be modelled only including several much higher frequencies: these deviations can be interpreted as flaring episodes in the jet, overlaid to the basic oscillating behavior of  $\sim 2500$  days. Such random variability is typical of BL Lac objects, so it is expected to be present. Using only the lowest frequency (which is the strongest) to fit the light curve, the best fit is achieved with a period of 2590 days and the rms deviation is 0.25, not dramatically larger than the 3-frequencies case. A formal Monte Carlo estimate of the period accuracy, made using the tools of Period04, gives  $2590 \pm 30$  days. A sinusoidal curve with period 2590 days and a decreasing trend of 0.053 mag/yr is reported in Fig. 4 to guide the eye.

We measured the source also on the POSS I digitized plate (1953-03-18, 103aO unfiltered, JD 34454) using our comparison sequence: the fit showed a rather large scatter (0.3 mag) and the source was at 16.05, which translates into  $B_J$  16.25 on our scale (see below the discussion of BZQJ1148+52). The same procedure on the POSS II plate (1991-02-09,

IIIaJ+GG395, JD 48296) gave a much better fit (rms 0.09) and the source was at  $B_J=16.19$ , similar to the GSC2.3 catalogue value of 16.04.

The POSS II observation is fully consistent with the Asiago light curve (see Fig. 4), while the POSS I observation is well below the extrapolation of the long term decreasing trend between JD 37,500 and JD 47,000: this is suggestive that this trend may be just part of an oscillating behavior with longer timescale. Further indications that this is actually the case come from the last points of the Asiago light curve (after JD 47000) and by more recent observations. One is from the SDSS (JD 52263,  $g=16.50$ ) which transforms into  $B_J=16.20$  in the GSC2.3 scale. Another is from our own photometry using the Vallinfreda 50cm telescope (JD 54995), which gives  $B=15.33 \pm 0.16$  and therefore tells that the source has returned to the very high state of the early 1960's (see Fig. 4).

#### BZQJ1148+5254

The spectrum of this source in the SDSS shows strong emission lines and a redshift  $z=1.632$ : it is therefore classified as a Flat Spectrum Radio Quasar in the Roma BZCat. The image is point-like in the SDSS, as expected for a high-redshift AGN. We found 67 plates with 103aO+GG13 and 19 plates with 103aO without filter taken with the 67/92 Schmidt, covering the time interval 24-01-1966 to 09-05-1994. The time distribution of the plates for this source is well suited to evaluate the systematic difference between the two dataset: the light curves derived separately were indeed rather similar, with the unfiltered points systematically brighter, as expected. To derive the systematic correction for the unfiltered values we averaged the magnitudes of the AGN in the time interval JD 44000 - 46500, (12 points without filter and 17 with GG13), obtaining  $\Delta M=0.20$ . This value was adopted also for the other two sources.

The Asiago light curve covers about 9000 days and shows a monotonic decreasing trend of about 1.8 mag (0.073 mag/year) with a slope quite similar to that of 1058+56.

The data are scattered around this trend, with no definite shorter time-scales. The photometric accuracy is however lower than in the case of 1058+56, due to the lower flux level of this source. As expected from the visual inspection, the DFT analysis did not show any remarkable frequency in the data besides the seasonal one year time scale of the observations. A couple of points definitely below the average (JD 43311 and 46478) are probably underestimated due to the lower quality of the plates.

On the POSS I plate (103aO unfiltered, 1950-03-20, JD 33360.85) we measured the source at  $15.98 \pm 0.10$ , which becomes  $B_J=16.18$  in the 103aO+GG13 system. The POSS I point is therefore brighter than the brightest one in the Asiago light curve, but definitely fainter than the straight extrapolation backwards of the observed trend. On the POSS II plate (IIIaJ+GG395, JD 49456.78) we measured the source at  $B_J 17.20 \pm 0.07$ . This observation is about 500 days after the last Asiago photographic point, and is roughly consistent with the general trend.

On the SDSS image (JD 52288) the source was at  $g=16.93$ , which becomes  $B_J=17.15$  on our scale. This is suggestive that the monotonic decrease has continued up to the year 2002.

Our CCD photometry from Vallinfreda (JD 54995), however, puts the AGN at  $B_J=16.6$ , indicating that the source has considerably brightened and is now back at the levels of 1960's.

BZBJ1209+4119

The source has an SDSS nearly featureless spectrum, and can be classified therefore as a BL Lac. In the SDSS database it is given a redshift  $z=0.377$  and the image is point-like.

We found 32 useful plates with 103aO+GG13 and 18 plates without filter in the 67/92 Schmidt archive. Most of the plates were centered on the star 2 CVN and some on 67

UMA. The dataset of two filter/emulsion combinations are not well mixed, so it is not easy to determine from them the systematic effect on the AGN magnitude. We used therefore the correction obtained from 1148+52 as discussed above. The source was too faint to be measurable on the small Schmidt films.

The Asiago light curve covers about 9500 days. The source is rather faint for the 67/92 Schmidt so the photometric accuracy is worse than for the other two sources. In this case a slow brightening trend (0.04 mag/year) seems to be present, with a large dimming episode around JD 45000. The rms deviations of the comparison stars of comparable faintness (S,G,T,Q, see Table 3) from their average values are anyway much smaller than that of the AGN, so that at least in a statistical sense the overall source variation is real. In the final part of the light curve the flux variation of the AGN is smaller, suggesting that part of the variations observed when the source was fainter may be due to its low signal/noise ratio; however, the faint comparison stars were always detected on the Asiago plates, so that we are confident that the low state of the AGN around JD 45000, recorded on several plates, is not just an artifact of photometric uncertainty.

Due to the low S/N ratio of the data, the low sampling frequency (on average 1 point every six months) and the presence of a single strong dimming feature in the light curve we do not think than a periodicity search is reliable.

On the digitized POSS I plate (1955-03-24, JD 35190) we measured the source at  $17.32 \pm 0.10$ , which converts into  $B_J=17.52$  in our system. On the POSS II plate (1996-03-19, JD 50161) we measured the source at  $B_J=17.57 \pm 0.04$ . On the SDSS image (JD 52731) the source is at  $g=17.98$ , which becomes  $B_J=18.28$  on our scale. We observed the source from Vallinfreda (JD 55040) in the R band, because it was too faint to be detected in B; in this case we used the SDSS r magnitudes for our comparison sequence stars and the source was at about 17.5, very near to the level of the SDSS observation ( $r=17.62$ ), suggesting that the

source did not change very much in the last years.

The slow historic trend shown by the Asiago plates does not extend outside the time window sampled by the Asiago observations. Indeed if we extrapolate the trend to the POSS I and POSS II epochs we would expect 18.1 and 16.8, while the source was at 17.5 in both plates. The two more recent observations of the SDSS and our own found the AGN in a much fainter state, at about 18.3, definitely not on the extrapolated trend (16.6) but rather at a flux level similar to the historic minimum recorded by six Asiago plates. Only a long time monitoring will tell us if such dimmings are a real characteristic of this source.

#### 4. Discussion

Pica et al. (1988) and Webb et al. (1988) studied the long-term behavior of several tens of AGNs with photographic plates for 15 to 20 years. For 61 sources they had enough data to morphologically classify their light curve in four types: Class I flickering without long term trend; Class II long term trend with small flickering; Class III long term and short term variability of comparable amplitude; Class IV rare outburst with stable flux level. In the Blazar sample of 22 sources of Webb et al. (1988) there is no significant difference in the frequency of the light curve classes between FSRQ and BL Lac objects, while a marked difference between Blazars and QSO exists in the Pica et al. (1988) sample of 39 sources, which includes a good number of radio steep spectrum Quasars and radio quiet QSO.

To have some physical insight of our sources we report in Table 7 some basic data: column 1 is the name, column 2 the Log(power) at 1.4 GHz, column 3 the absolute R magnitude computed from the USNO B1 catalogue magnitude and literature redshift, column 4 the Radio/Optical flux ratio, column 5 the NIR spectral slope from the JHK magnitudes in the 2MASS catalogue, column 6 the optical spectral slope from the SDSS

data. We remark that, at variance with the other two sources, the spectral slopes computed for BZQJ1148+52 have a very poor  $\chi_r^2$  and are therefore marked with ”:”. Actually the spectrum of this source cannot be well fitted with a power law in neither of the two explored ranges, probably due to the strong emission lines (e.g. C IV equivalent width is 77 Å) and of the UV bump which falls in the optical due to the source redshift.

It is apparent from this Table that our three sources are flat-spectrum radio-loud objects (Radio/Optical flux ratio  $\geq 10$ ) but have different absolute luminosities and show substantially different behaviors in their optical light curve. The strong-lined object is the brightest both in the radio and optical bands. Only BZBJ1058+56 was detected in Gamma-rays by Fermi-LAT (Abdo et al. 2009) and possibly also by EGRET (Bloom et al. 2000).

From the point of view of the overall Spectral Energy Distribution, a much used tool for the classification of Blazars is the  $\alpha_{ro} - \alpha_{ox}$  diagram (Padovani and Giommi 1995). On this diagram the Blazars mainly occupy two areas: a horizontal branch and a diagonal branch; a diagonal line of negative slope -1 is a line of constant Radio/X-ray flux ratio. The line at  $\alpha_{rx}=0.75$  is the formal border between HBL and LBL sources (Padovani and Giommi 1995). Extreme HBL sources are located at the left side of the horizontal branch, extreme LBL at the upper side of the diagonal branch. For a Synchrotron Self Compton emission model, as the peak of the synchrotron emission of a Blazar moves from lower ( $10^{13}$ Hz) to higher ( $10^{17}$ Hz) frequencies the location of the source on this diagram moves from the upper left corner to the lower right one along the diagonal line and then back to the left along the horizontal branch.

We report in Fig. 7 this diagram for the sources in the Roma BZCat, with the positions of our three objects marked. BZBJ1209+41 and BZQJ1148+52 have  $\alpha_{rx}$  larger than 0.75, and are located in the diagonal branch, with BZBJ1209 being the most radio loud.

BZBJ1058+56 is already on the horizontal branch and is an HBL, as discussed by Donato et al. (2005) also on the basis of BeppoSAX X-ray spectra. None of them is however an extreme case.

The long-term optical light curves of our three sources are rather different. As a general remark, the overall amplitude variability is anticorrelated with the intrinsic power.

BZBJ1058+56 showed regular oscillations of about 1 mag amplitude, with timescale of  $\sim 2300$  days, over a monotonic decreasing trend of 0.07 mag/year; it can be classified as Class III and is the source with the larger variability. Its historic light curve contains 5 outbursts sampled by the Asiago plate archive; this source seems therefore an interesting case of quasi-periodic BL Lac. Further multiwavelength monitoring of this source, should be performed.

BZQJ1148+52 showed a monotonic decreasing trend with a slope similar to 1058+56 but without the oscillating behavior: the detected short-term variability is comparable to our photometric uncertainty, so no firm conclusions can be derived on their time scale. It can be put into Class II. It showed a substantially smaller variability than the other two BL Lacs, both on short and long time scales.

BZBJ1209+41 showed a slight increasing trend (0.04 mag/year) with large dips in its light curve: it is therefore quite unusual (the opposite of Class I) and deserves further monitoring. Unfortunately it is not bright enough to be easily followed with small telescopes.

When a time interval of about 50 years is considered, all the long term trends detected in the time window of 27 years sampled by the Asiago plates do not seem to hold, so that they might be considered just as part of longer variability trends.

Which processes can be behind these secular trends? Both physical processes and

geometrical effects can be at work: in the first case one can imagine a monotonic variation of the number of radiating electrons, or of the average ambient magnetic field; in the second case, a change in the Doppler boosting factor along our line of sight due to the jet precession. The latter possibility can be considered as an indicator of a massive black hole binary system in the nuclear region (see e.g. Romero et al. 2003).

If we interpret the long term trends of our three sources as due to a slow precession of the jet, as in was supposed to be in the case of S5 0716+71 (Nesci et al. 2005), then the periodicity should be of several  $10^4$  days and therefore comparable to (or even larger than) the human lifetime. This poses a strong challenge because observations must be accumulated for several tens of years before any firm conclusion can be reached. A further difficulty for the data interpretations, if the monitoring is not dense enough, could be the occurrence of fast and/or large occasional outbursts/dips, which can mask the long-term trends.

A strong support to confirm the precession model could come from imaging at high radio frequencies with VLBI techniques, which could detect monotonic variations in the jet direction and/or at lower frequencies showing residuals of radio emission in regions involved by the crossing of the jet in the past (see e.g. Massaro et al. 2004).

Finally, we remark that the detection of the quasi-periodicity of BZB J1058+56 from the Asiago plates suggests that further discoveries could be made using other, still unexplored, photographic plate archives.

We thank the Asiago Observatory and the Department of Astronomy of Padova University for hospitality for the plate archive search, and Alfredo Segafredo for scanning part of the plates. The Guide Star Catalogue-II is a joint project of the Space Telescope Science Institute and the Osservatorio Astronomico di Torino (OATo/INAF). This research

made use of the CDS (Strasbourg), NED (NASA /IPAC Extragalactic Database) and SDSS (Sloan Digital Sky Survey) databases.

## REFERENCES

- Abdo, A. A. et al. 2009, *ApJ*, 700, 597
- Adelman-McCarthy et al. 2008, *ApJS*, 175, 297. The Sixth Data Release of the Sloan Digital Sky Survey
- Bade, N., Beckmann, V., Douglas, N. G., Barthel, P. D., Engels, D., Cordis, L., Nass, P., & Voges, W. 1998, *A&A*, 334, 459
- Bloom, S. D., Hallum, J., Terasranta, H., & Tornikoski, M. 2000 *ApJ*529, 675
- Ciaramella, A., Bongardo, C., Aller, H.D., Aller, M.F., De Zotti, G., et al. 2004 *A&A*, 419, 485
- Collinge M. J.; Strauss, M. A.; Hall, P.B. et al. 2005, *AJ*, 129, 2542
- Donato, D., Sambruna, R. M., & Gliozzi, M. 2005, *A&A*, 433, 1163
- Giveon, U., Maoz, D., Kaspi, S., Netzer, H., & Smith, P.S. 1999, *MNRAS*, 306, 637
- Kadler, M., Hughes, P.A., Ros, E., Aller, M.F., & Aller, H.D. 2006, *A&A*, 456, L1
- Laurent-Muehleisen, S. A., Kollgaard, R. I., Ciardullo, R., Feigelson, E. D., Brinkmann, W., & Seibert, J. 1998, *ApJS*, 118, 127
- Lenz, P., Breger, M., 2005, *CoAst* 146, 53
- Marcha M. J. M., Browne, I. W. A., Impey, C. D., & Smith, P. S. 1996, *MNRAS*, 281, 425
- Massaro, E., Mantovani, F., Fanti, R., Nesci, R., Tosti, G., & Venturi, T. 2001, *A&A*, 374, 435
- Massaro, E., Mantovani, F., Fanti, R. et al. 2004, *A&A*, 423, 935

- Massaro, E., Giommi, P., Leto, C., et al. 2009, *A&A*, 495, 691
- Nesci, R., Massaro, E., Rossi, C., Scavi, S., Maesano, M., & Montagni, F. 2005, *AJ*, 130, 1466
- Nesci, R., Mandalari, M., & Gaudenzi, S., 2007, *AJ*, 133, 965
- Padovani, P., & Giommi, P., 1995, *ApJ*, 444, 567
- Pica, A.J., Smith, A.G., Webb, J.R., Leacock, R.J., Clements, S., & Gombola, P.P. 1998, *AJ*, 96, 1215
- Qian, S.J., Kudryavtseva, N.A., Britzen, S., Krichbaum, T.P., Witzel, A, et al. 2007 *ChJAA*, 7, 364
- Raiteri, C. M., Villata, M., Chen, W. P., et al. 2008, *A&A*, 485, L17
- Raiteri, C.M., Villata, M., Tosti, G., Nesci, R., et al. 2003 *A&A*, 402, 151
- Romero, G. E., Fan, Jun-Hui, & Nuza, S. E. 2003, *ChJAA* , 3, 516
- Sharov, A., S., 1995, *Astronomy Letters* 21, 447.
- Sillanpää, A., Haarala, S., Valtonen, M. J., Sundelius, B., & Byrd, G. G. 1988, *ApJ*, 325, 628
- Sowards-Emmerd, D., Romani, R.W., Michelson, P.F., Healey, S.E., & Nolan, P.L. 2005, *ApJ*, 626, 95
- Trager, S. C., Worthey, G., Faber, S. M., Burstein, D., & Gonzalez, J. J. 1998, *ApJS*, 116,1
- Valtonen, M. J., Nilsson, K., Villforth, C., Lehto, H. J., Takalo, L. O., et al. 2009, *ApJ*, 698, 781 Lindfors, E.; Sillanp, A.; Hentunen, V.-P.; Mikkola, S.; Zola, S.;

Webb, J.R., Smith, A.G., Leacock, R.J., Fitzgibbons, G.L., Gombola, P.P., & Shepherd,  
D.W. 1998, AJ, 95, 374

Table 1. Comparison stars in the field of BZB J1058+56

RA(2000)	DEC(2000)	ident.	$B_J$ mag	B/Asiago	rms
164.27350	56.53899	B	16.55	16.62	0.08
164.32579	56.43882	C	17.72	17.66	0.08
164.34494	56.44861	E	17.68	17.74	0.09
164.35300	56.38940	D	16.09	16.00	0.09
164.38134	56.46707	F	17.22	17.29	0.09
164.47731	56.45302	I	15.61	15.80	0.07
164.47977	56.58929	J	16.16	16.38	0.08
164.60784	56.44601	K	16.58	16.65	0.08
164.61842	56.54285	L	17.01	16.98	0.09
164.62266	56.43455	M	15.58	15.57	0.05
164.65048	56.34049	N	15.19	15.33	0.06
164.65070	56.53979	O	15.94	15.92	0.06
164.67445	56.50317	P	17.73	17.67	0.08
164.69448	56.39540	Q	15.43	15.31	0.06
164.75473	56.33177	R	17.12	17.03	0.07
164.80188	56.49624	S	17.71	17.60	0.08
164.82489	56.33905	T	15.50	15.43	0.09
164.84320	56.37278	U	17.18	17.32	0.13
164.97340	56.44394	Y	16.18	16.02	0.16
164.97473	56.48899	W	17.43	17.35	0.14



Table 2. Comparison stars in the field of BZB J1148+52

RA(2000)	DEC(2000)	ident.	$B_J$ mag	B/Asiago	rms
177.21235	52.93091	B	16.14	16.20	0.09
177.28202	52.84490	E	17.34	17.27	0.12
177.43974	52.97246	F	17.87	17.77	0.14
177.43928	52.98250	G	17.77	17.78	0.14
177.49464	52.97587	H	16.29	16.22	0.11
177.50878	52.98667	I	17.40	17.48	0.15
177.44770	53.04665	L	16.67	16.90	0.12
177.02230	52.99680	M	17.80	17.83	0.13
177.09700	53.01454	N	17.81	17.70	0.13
177.10528	52.90447	P	15.66	15.48	0.05
177.13476	52.89412	Q	15.92	16.05	0.13
177.19421	53.00136	S	15.98	15.95	0.09
177.25626	53.02330	T	17.35	17.27	0.14
176.96426	52.95703	U	15.29	15.43	0.08
177.15185	52.84147	V	16.94	16.92	0.12

Table 3. Comparison stars in the field of BZB J1209+41

RA(2000)	DEC(2000)	ident.	$B_J$ mag	B/Asiago	rms
182.48757	41.35025	B	17.02	17.09	0.09
182.38187	41.43152	D	17.00	17.06	0.08
182.41075	41.24259	E	16.23	16.30	0.07
182.23561	41.42514	F	16.98	17.09	0.09
182.39451	41.35070	G	18.34	18.24	0.16
182.38566	41.35420	H	16.07	16.20	0.12
182.19538	41.40745	I	16.59	16.67	0.07
182.20402	41.23872	J	14.97	14.97	0.11
182.33838	41.27927	M	15.36	15.33	0.07
182.29515	41.21913	O	17.49	17.40	0.09
182.35833	41.18281	P	15.34	15.29	0.06
182.29730	41.24304	Q	18.63	18.42	0.16
182.37593	41.18086	R	17.83	17.81	0.13
182.37925	41.37451	S	18.39	18.02	0.12
182.44092	41.37890	T	18.03	18.39	0.21
182.21330	41.44316	W	18.01	17.91	0.16
182.20821	41.44291	Z	17.83	17.86	0.12

Table 4. Relevant data for our Blazar sample.

Name	$\log(P_{1.4})$	$M_R$	R/Opt	$\alpha_{JHK}$	$\alpha_{ugriz}$
BZBJ1058+56	24.9	-25.0	29.5	-0.58	-1.35
BZQJ1148+52	26.8	-28.9	63.1	-0.16:	-0.97:
BZBJ1209+41	25.9	-24.2	561	-1.13	-1.23

Table 5. Historic  $B$  magnitudes of BZB1058+5621 from the Asiago archive

Plate	Filter	JD	$B_J$	err
OSC 0712	none	34454.7917	16.25	0.35
S40 02499	PANC	37694.2986	14.92	0.06
S40 02529	PANC	37696.4341	14.83	0.08
S40 02552	PANC	37698.4230	15.55	0.10
S40 02605	PANC	37702.3035	14.73	0.08
S40 02615	PANC	37707.5452	14.84	0.09
S40 02634	PANC	37719.3348	15.00	0.10
S40 02659	PANC	37732.3153	14.88	0.08
S40 02691	PANC	37753.4709	14.93	0.08
S40 02708	PANC	37760.3709	14.92	0.07
S40 02732	PANC	37763.3938	14.83	0.11
S40 02755	PANC	37780.3271	15.06	0.09
S40 02781	PANC	37786.3313	14.74	0.07
S40 02831	PANC	37817.4757	14.67	0.05
S40 02845	PANC	37821.4848	14.92	0.21
S40 02861	PANC	37824.5278	15.10	0.12
S40 02896	PANC	37843.4882	14.74	0.16
S40 03291	PANC	37972.6174	15.43	0.09
S40 03324	PANC	37992.5924	15.22	0.15
S40 03360	PANC	37998.5827	15.54	0.12
S40 03400	PANC	38001.6591	15.27	0.10
S40 03435	PANC	38005.6243	15.35	0.08
S40 03504	PANC	38020.5355	15.47	0.09
S40 03600	PANC	38049.5528	15.41	0.09
S40 03675	PANC	38055.5382	15.41	0.06

Table 5—Continued

Plate	Filter	JD	$B_J$	err
S40 03741	PANC	38081.4813	15.34	0.08
S40 03817	PANC	38089.6466	15.20	0.10
S40 03864	PANC	38106.3757	15.20	0.08
S40 03908	PANC	38139.3243	15.35	0.14
S40 03946	PANC	38166.4146	15.51	0.10
S40 04007	PANC	38193.3931	15.06	0.06
S40 04055	PANC	38207.5049	15.40	0.08
S40 04138	none	38316.6216	15.62	0.12
S40 04235	PANC	38346.6146	15.40	0.07
S90 00060	none	39093.6000	15.41	0.04
S90 00182	none	39168.5667	15.06	0.04
S90 00228	none	39199.4076	15.64	0.11
S90 00473	none	39475.6201	15.28	0.06
S90 00573	none	39506.6292	15.54	0.10
S90 00635	none	39587.3840	15.35	0.08
S90 00651	none	39609.3285	15.34	0.06
S90 00690	none	39622.4472	15.18	0.04
S90 01295	none	39864.5653	15.48	0.09
S90 01466	GG13	39914.4542	15.71	0.14
S90 01571	GG13	39942.4750	15.56	0.07
S90 01587	GG13	39947.3979	15.68	0.09
S90 01623	GG13	39972.3958	15.62	0.06
S40 06837	PANC	40150.6035	15.34	0.11
S40 06838	none	40150.6146	15.14	0.34
S90 02203	GG13	40260.4757	15.39	0.05

Table 5—Continued

Plate	Filter	JD	$B_J$	err
S90 02225	GG13	40263.4660	15.30	0.12
S90 02230	GG13	40267.5819	15.12	0.08
S90 02246	GG13	40271.4701	15.31	0.04
S90 02276	GG13	40290.3903	15.81	0.04
S40 07158	PANC	40319.4063	15.20	0.13
S90 02289	GG13	40319.4861	15.30	0.05
S90 02301	GG13	40321.5708	15.33	0.03
S90 02315	GG13	40322.4868	15.30	0.04
S40 07220	PANC	40327.3757	15.46	0.13
S90 02350	GG13	40329.5382	15.51	0.03
S40 07301	PANC	40392.4237	15.49	0.11
S40 07302	PANC	40392.4333	15.49	0.12
S40 07321	PANC	40412.4341	15.60	0.12
S40 07494	PANC	40505.6098	15.68	0.13
S90 04272	none	40979.4882	16.34	0.06
S90 04212	none	40999.5375	16.10	0.09
S90 04213	none	40999.5521	16.06	0.06
S90 05376	none	41446.3486	15.82	0.19
S90 07799	GG13	42425.4889	15.53	0.05
S90 07880	GG13	42459.5257	15.46	0.05
S90 07895	GG13	42514.3826	15.59	0.06
S90 08415	GG13	42833.4562	15.81	0.10
S90 08453	GG13	42863.4681	15.84	0.03
S90 08925	GG13	43187.3549	16.36	0.15
S90 08949	GG13	43226.4403	16.19	0.10

Table 5—Continued

Plate	Filter	JD	$B_J$	err
S90 09446	GG13	43540.3833	16.30	0.11
S90 09479	GG13	43569.3611	16.49	0.09
S90 09818	GG13	43843.5243	16.16	0.09
S90 09991	GG13	43966.5528	16.45	0.05
S90 10300	GG13	44203.5389	16.38	0.07
S90 10318	GG13	44220.4896	16.57	0.04
S90 10368	none	44250.3910	16.67	0.13
S90 10393	none	44273.3826	16.35	0.11
S90 10467	none	44344.4153	16.18	0.07
S90 10780	none	44611.5354	15.73	0.06
S90 10816	none	44630.3521	15.97	0.07
S90 10864	none	44636.4799	15.88	0.08
S90 11238	none	44931.5403	15.62	0.09
S90 11273	none	44941.4799	15.61	0.11
S90 11328	GG13	44988.4722	16.11	0.06
S90 11416	GG13	45026.5333	15.85	0.05
S90 11462	GG13	45053.4306	15.91	0.06
S90 11535	GG13	45105.4257	15.68	0.07
S90 11847	none	45343.4743	16.01	0.06
S90 11934	none	45367.4444	16.16	0.06
S90 11981	none	45398.4174	16.12	0.08
S90 12029	none	45407.4458	16.06	0.05
S90 12057	none	45440.3674	16.24	0.09
S90 12307	GG13	45647.5139	17.05	0.05
S90 12453	GG13	45766.5125	16.88	0.05

Table 5—Continued

Plate	Filter	JD	$B_J$	err
S90 12483	GG13	45814.3646	17.20	0.05
S90 12669	GG13	46027.5111	16.67	0.04
S90 12748	GG13	46062.4549	16.71	0.09
S90 13784	GG13	46909.4167	16.77	0.05
S90 13998	GG13	47184.5174	16.77	0.07
S90 14019	GG13	47205.4882	16.56	0.04
S90 14052	GG13	47212.5042	16.54	0.04
S90 14066	GG13	47231.3722	16.62	0.03
S90 14413	GG13	47556.4083	16.44	0.04
S90 14427	GG13	47558.4354	16.40	0.05
S90 14984	GG13	48275.5528	16.30	0.09
OSC SJ03821	GG395	48296.8333	16.19	0.07
S90 15014	GG13	48301.4118	16.34	0.12
S90 15031	GG13	48329.3840	16.46	0.05
S90 15136	GG13	48628.5125	15.98	0.05
SDSS ccd	g	52263.0000	16.20	0.05
VALLIN ccd	B	54995.3625	15.33	0.16

Table 6. Historic  $B_J$  magnitudes of BZBJ1148+5254 from the Asiago archive

Plate	Filter	JD	$B_J$	err
OSC O59	none	33360.8611	16.18	0.10
S90 00201	none	39181.4630	16.32	0.06
S90 00235	none	39201.4450	16.34	0.08
S90 00484	none	39477.5120	16.45	0.07
S90 00561	none	39503.4980	16.29	0.06
S90 00625	GG13	39565.6040	16.40	0.10
S90 00654	none	39610.3470	16.51	0.06
S90 01482	GG13	39938.3600	16.43	0.05
S90 02382	GG13	40362.5150	16.48	0.08
S90 02389	GG13	40364.4920	16.38	0.10
S90 02403	GG13	40375.3970	16.63	0.11
S90 02404	GG13	40386.3900	16.53	0.09
S90 02405	GG13	40387.3900	16.55	0.10
S90 02420	GG13	40406.4180	16.88	0.10
S90 04273	GG13	41040.4990	16.74	0.06
S90 04301	GG13	41057.4030	16.79	0.04
S90 05319	none	41393.4840	16.91	0.12
S90 07151	GG13	42134.3530	16.76	0.08
S90 07155	GG13	42149.4560	16.82	0.07
S90 07870	GG13	42453.5000	16.91	0.05
S90 07893	GG13	42511.5220	16.82	0.04

Table 6—Continued

Plate	Filter	JD	$B_J$	err
S90 07898	GG13	42514.4610	16.85	0.05
S90 08416	GG13	42835.4810	16.96	0.03
S90 08532	GG13	42889.4340	16.73	0.10
S90 08854	GG13	43140.5700	16.99	0.04
S90 08928	GG13	43191.5140	16.91	0.05
S90 08951	GG13	43226.4930	16.89	0.05
S90 09444	GG13	43311.3970	16.73	0.11
S90 09472	GG13	43553.5480	16.78	0.09
S90 09486	GG13	43631.3660	16.95	0.05
S90 09838	GG13	43846.5620	16.75	0.09
S90 09910	GG13	43905.5020	16.81	0.04
S90 09918	GG13	43926.4350	17.04	0.08
S90 09943	GG13	43936.4310	16.96	0.05
S90 09961	GG13	43960.3160	16.83	0.06
S90 09967	GG13	43962.3930	16.79	0.06
S90 09969	GG13	43963.3750	16.85	0.05
S90 09984	GG13	43966.4140	16.95	0.11
S90 10000	GG13	43986.4000	16.89	0.07
S90 10028	GG13	44013.4060	16.86	0.10
S90 10061	GG13	44017.4480	16.76	0.09
S90 10309	GG13	44219.4630	16.92	0.07

Table 6—Continued

Plate	Filter	JD	$B_J$	err
S90 10372	none	44252.3540	17.13	0.18
S90 10391	none	44275.3410	17.09	0.11
S90 10817	none	44630.3770	17.03	0.10
S90 10887	none	44640.4960	16.79	0.09
S90 11240	none	44931.6040	16.87	0.05
S90 11305	GG13	44972.6130	16.88	0.06
S90 11329	GG13	44988.4990	16.99	0.05
S90 11452	GG13	45048.4390	17.02	0.10
S90 11481	GG13	45055.4430	16.90	0.04
S90 11502	GG13	45086.4250	17.00	0.06
S90 11855	none	45344.4910	17.05	0.07
S90 11942	none	45378.4680	16.92	0.05
S90 12028	none	45407.4260	17.07	0.06
S90 12059	none	45440.4140	16.97	0.09
S90 12455	GG13	45766.5700	17.10	0.08
S90 12482	GG13	45813.4320	16.87	0.11
S90 12485	GG13	45814.4090	17.02	0.10
S90 12700	none	46035.5630	17.00	0.07
S90 12711	GG13	46049.3910	16.77	0.12
S90 12746	GG13	46061.4730	17.02	0.06
S90 12829	GG13	46171.3960	17.09	0.10

Table 6—Continued

Plate	Filter	JD	$B_J$	err
S90 13211	none	46419.5460	17.12	0.09
S90 13231	GG13	46442.5120	17.16	0.06
S90 13292	GG13	46478.4550	17.40	0.07
S90 13303	GG13	46495.4500	17.18	0.10
S90 13335	none	46563.3790	17.06	0.08
S90 13602	GG13	46770.5420	17.09	0.04
S90 13756	GG13	46879.4530	17.01	0.05
S90 13779	GG13	46908.3580	17.07	0.04
S90 13796	none	46937.3680	17.23	0.12
S90 14025	GG13	47208.3990	17.24	0.04
S90 14069	GG13	47231.4520	17.02	0.03
S90 14422	GG13	47560.5290	17.17	0.03
S90 14487	GG13	47586.4520	17.05	0.05
S90 14516	GG13	47593.3880	17.19	0.05
S90 14535	GG13	47651.3990	17.11	0.07
S90 15374	GG13	48987.4730	17.31	0.10
OSC SJ05730	GG395	49456.7896	17.20	0.05
SDSS ccd	b	52288.0000	17.17	0.03
VALLIN ccd	B	54995.3500	16.61	0.09



Table 7. Historic  $B_J$  magnitudes of BZBJ1209+4119 from the Asiago archive

Plate	Filter	JD	$B_J$	err
OSC O1367	none	35190.8611	17.50	0.10
S90 00184	none	39171.5993	18.10	0.08
S90 00237	none	39201.4681	18.15	0.13
S90 00297	none	39287.4389	17.78	0.17
S90 00631	none	39585.4861	18.00	0.09
S90 00648	none	39593.3966	18.15	0.12
S90 00692	none	39622.4952	17.76	0.13
S90 01519	GG13	39942.5063	17.54	0.08
S90 05377	none	41449.3452	17.54	0.08
S90 06896	GG13	42016.6196	17.62	0.21
S90 07667	none	42391.5167	17.73	0.05
S90 07748	GG13	42402.5980	17.77	0.10
S90 07851	GG13	42451.5091	18.10	0.06
S90 07905	GG13	42515.4299	18.02	0.07
S90 07942	GG13	42541.4966	17.66	0.07
S90 07976	GG13	42569.3959	17.80	0.07
S90 08368	GG13	42817.5660	17.87	0.04
S90 08461	GG13	42866.4771	17.70	0.08
S90 08523	GG13	42872.5396	17.49	0.08
S90 08530	GG13	42889.3917	17.61	0.13
S90 08567	GG13	42904.5466	17.81	0.12

Table 7—Continued

Plate	Filter	JD	$B_J$	err
S90 08907	GG13	43165.4924	17.65	0.13
S90 08922	GG13	43189.5119	17.34	0.05
S90 08954	GG13	43226.5675	17.68	0.07
S90 09013	GG13	43284.4786	17.41	0.08
S90 09034	GG13	43307.4015	17.60	0.15
S90 09499	GG13	43657.4376	18.00	0.11
S90 09928	GG13	43927.5189	18.21	0.04
S90 10052	GG13	44016.4473	17.86	0.12
S90 10346	none	44226.5035	17.98	0.13
S90 10906	none	44642.5404	17.54	0.09
S90 10947	none	44691.4446	17.42	0.14
S90 11337	GG13	44989.4911	18.61	0.08
S90 11453	GG13	45048.4675	18.15	0.09
S90 11482	GG13	45055.4723	18.36	0.09
S90 11518	GG13	45088.5147	18.48	0.10
S90 11877	none	45347.4869	18.69	0.08
S90 11885	none	45350.4841	18.87	0.12
S90 11989	none	45399.4445	17.98	0.05
S90 12040	none	45412.4348	17.65	0.10
S90 12055	none	45439.5035	17.56	0.09
S90 12441	GG13	45738.4689	17.34	0.11

Table 7—Continued

Plate	Filter	JD	$B_J$	err
S90 12493	GG13	45816.5279	17.93	0.10
S90 14075	GG13	47232.4258	17.14	0.07
S90 14382	GG13	47535.5251	17.05	0.09
S90 14442	GG13	47564.4377	17.34	0.14
S90 14994	GG13	48277.5331	17.14	0.15
S90 15022	GG13	48306.5585	16.88	0.09
S90 15043	GG13	48331.4518	17.27	0.11
OSC SJ06694	GG395	50161.9111	17.50	0.10
SDSS ccd	b	52731.0000	18.30	0.05
VALLIN ccd	B	55040.3560	18.30	0.20

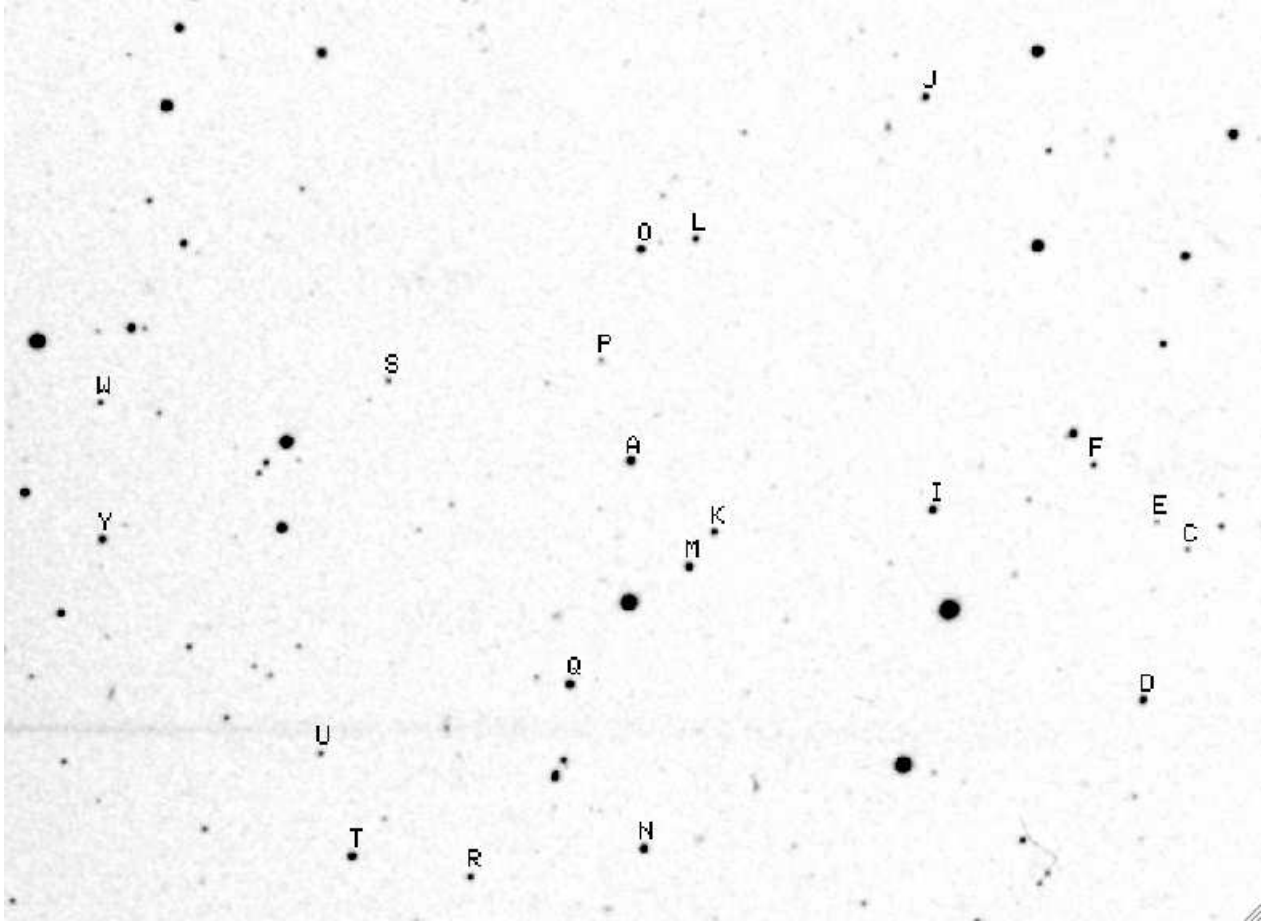


Fig. 1.— Comparison stars in the field of BZBJ1058+56: the reference stars are marked with letters starting from B, the AGN is marked with A. North is up and East to the left. Field of view about 16' in DEC.

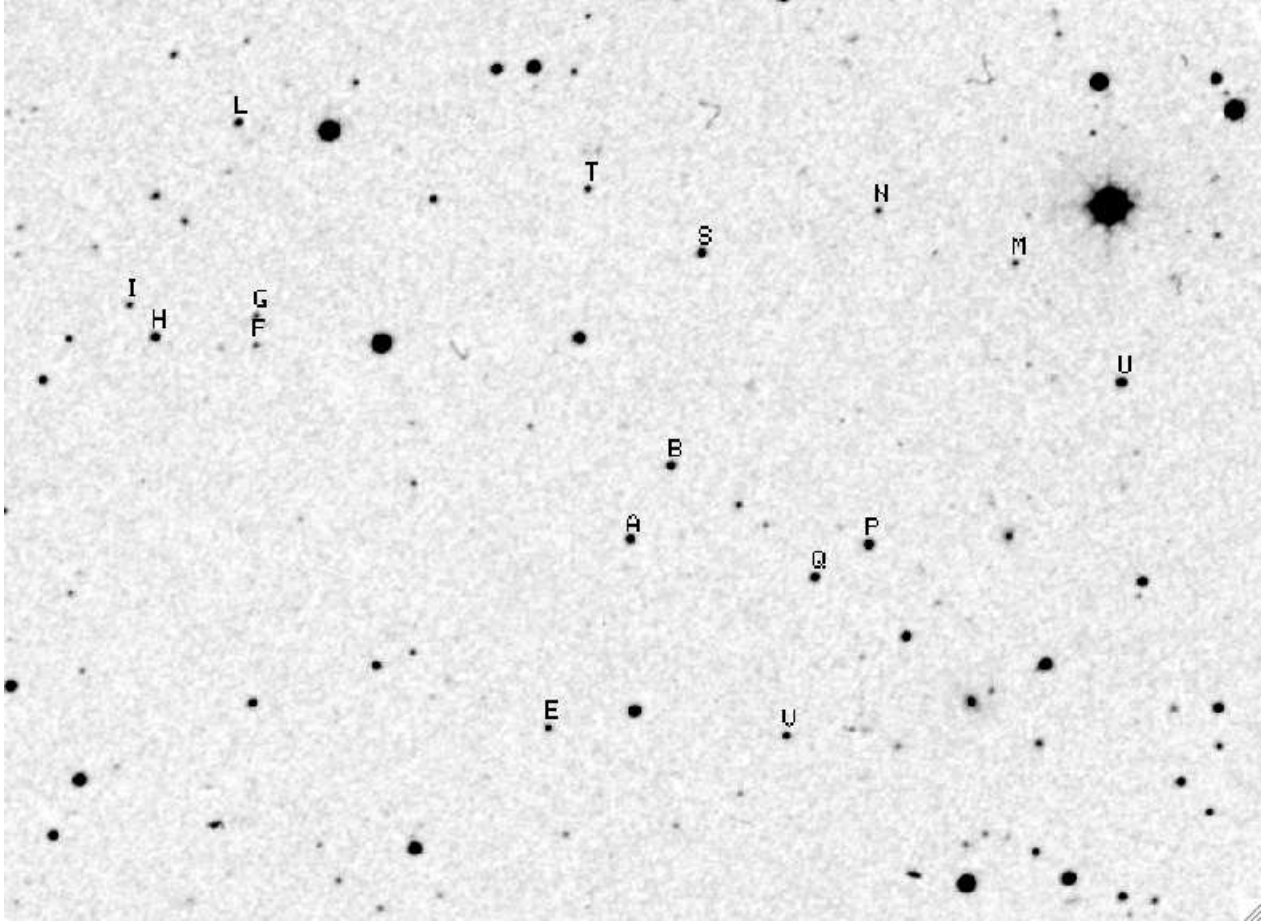


Fig. 2.— Comparison stars in the field of BZBJ1148+52: the reference stars are marked with letters starting from B, the AGN is marked with A. North is up and East to the left. Field of view about 17' in DEC.

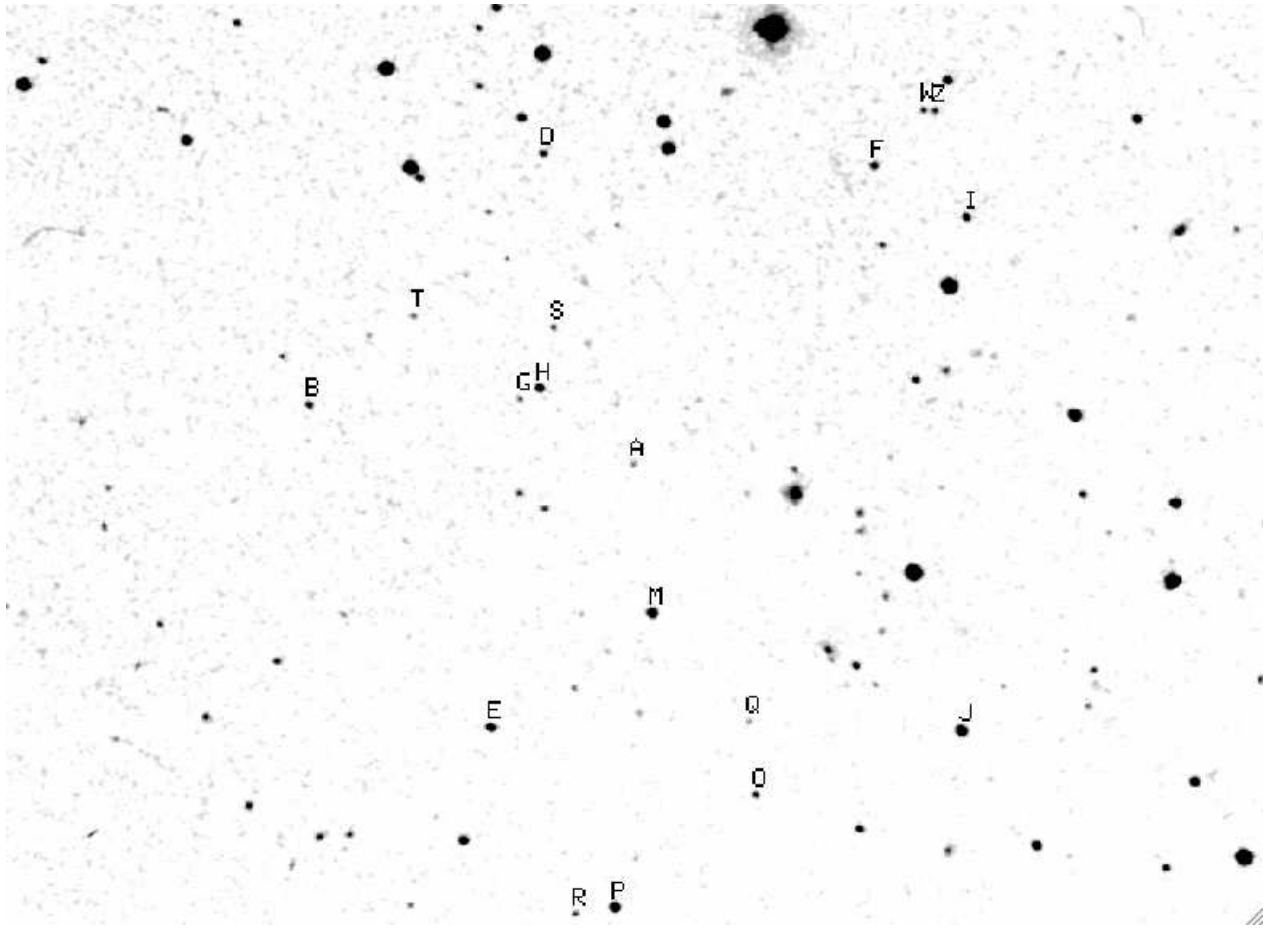


Fig. 3.— Comparison stars in the field of BZBJ1209+41: the reference stars are marked with letters starting from B, the AGN is marked with A. North is up and East to the left. Field of view about 18' in DEC.

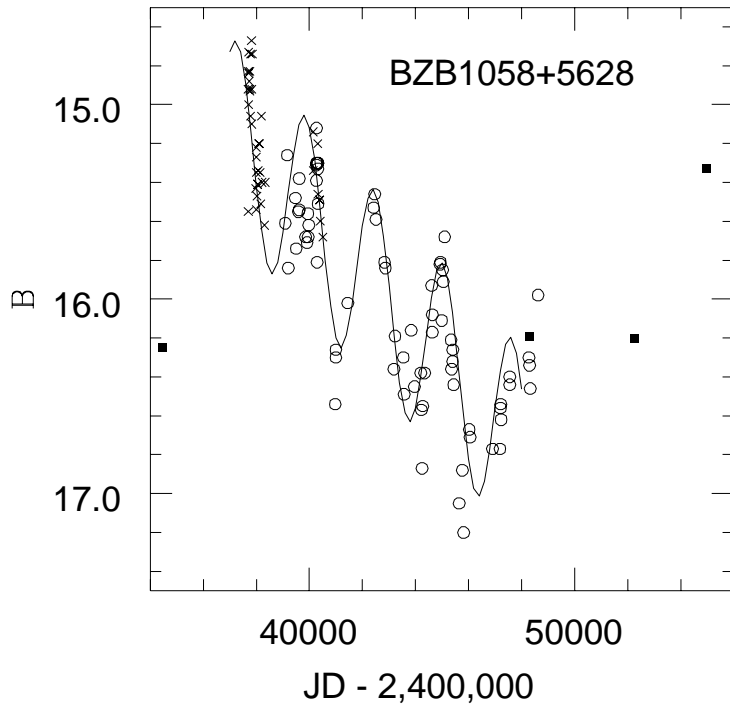


Fig. 4.— The historic light curve in the  $B$  band of BZBJ1058+56. from March 1953 to June 2009. Filled circles are data from the Asiago 67/92cm Schmidt plates; crosses from the Asiago 40/50cm Schmidt corrected for the zero point shift; open squares other data. Error bars are omitted for clarity. A sinusoidal line with a period of 2590 days and a monotonic

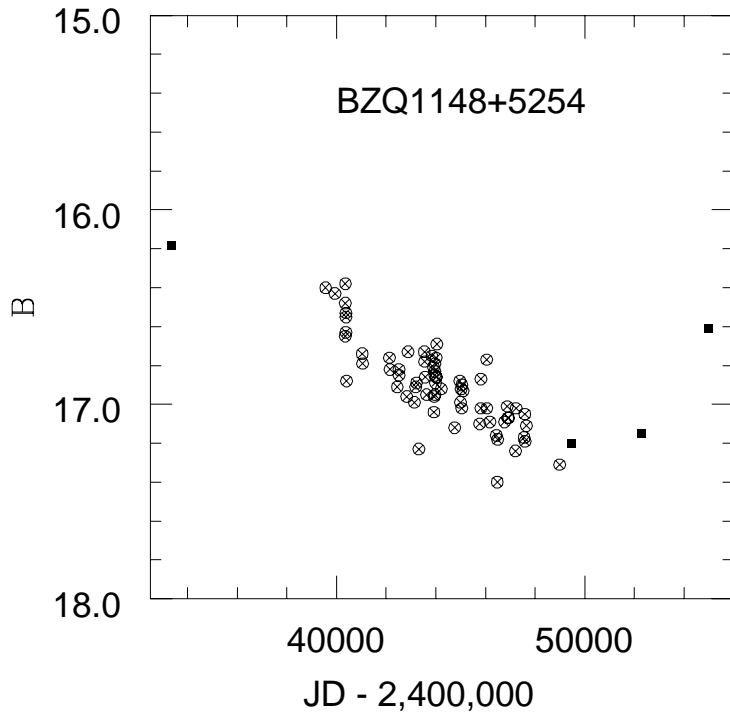


Fig. 5.— The historic light curve in the  $B$  band of BZBJ1148+52. from March 1950 to June 2009. Filled circles are data from the Asiago 67/92cm Schmidt plates with GG13 filter; crosses are unfiltered data from the same telescope corrected for the zero point shift; open squares are other data. Error bars are omitted for clarity.



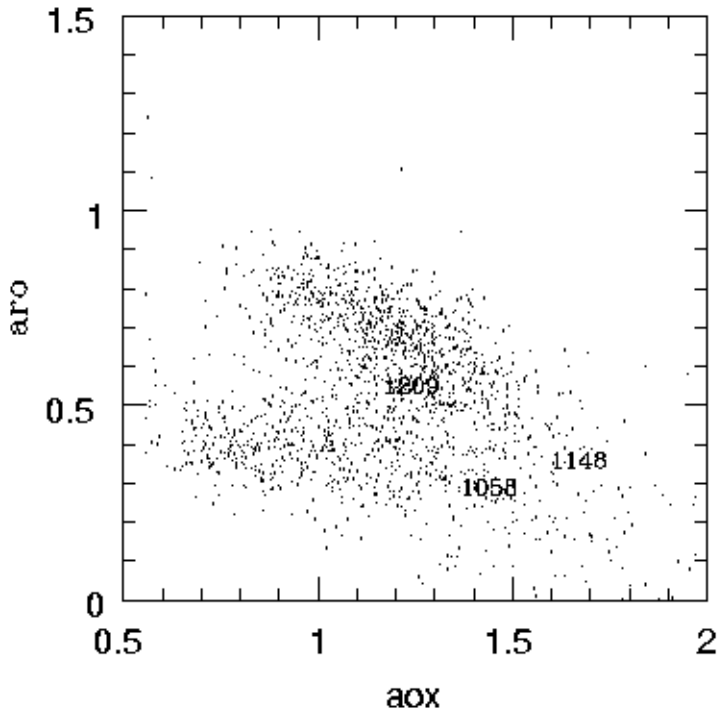


Fig. 7.— The  $\alpha_{ro} - \alpha_{ox}$  plot for the sources in the Roma BZCat. The approximate positions of the three sources of this paper are marked.